Ferrimagnetism in PrCoO_{3} epitaxial films

Virat V. Mehta, Shameek Bose, Jodi M. Iwata-Harms, Elke Arenholz, C. Leighton, and Y. Suzuki

Phys. Rev. B **87**, 020405 — Published 15 January 2013

DOI: 10.1103/PhysRevB.87.020405

Ferrimagnetism in $PrCoO_3$ epitaxial films

Virat V. Mehta,[1,2] Shameek Bose,[3] Jodi M. Iwata-Harms,[1]
Elke Arenholz,[4] Christopher Leighton,[3] and Yuri Suzuki[1,2,5]

[1]*Dept. of Materials Science and Engineering, University of California, Berkeley, CA 94720, USA*
[2]*Materials Sciences Division, Lawrence Berkeley National Laboratory, Berkeley, CA 94720, USA*
[3]*Dept. of Chemical Engineering and Materials Science, University of Minnesota, Minneapolis, MN 55455, USA*
[4]*Advanced Light Source, Lawrence Berkeley National Laboratory, Berkeley, CA 94720, USA*
[5]*Dept. of Applied Physics and Geballe Lab for Advance Materials, Stanford University, Stanford, CA 94305, USA*

(Dated: December 14, 2012)

We demonstrate the stabilization of a *ferri*magnetic ground state in epitaxial films of $PrCoO_3$ grown on $SrTiO_3$ (001) substrates, in stark contrast to paramagnetic behavior observed in bulk. Heteroepitaxial strain is found to induce long-range ordering of the Co ions, which we deduce to be in a high spin state. The ferromagnetic ordering of the CoO_6 array is accompanied by ordering of the Pr sub-lattice in an antiparallel orientation to the Co. The ordering of the Pr sub-lattice provides evidence for significant Co-Pr exchange likely facilitated by the presence of high spin Co.

PACS numbers: 75.30.Et, 75.47.Lx, 75.50.Gg, 75.70.Ak

Spin state transitions in condensed matter systems have been extensively studied in order to understand the underlying correlated electron behavior and competing degrees of freedom that determine the ground state.[1,2] The ability to access different spin states through parameters such as temperature and strain could create new functionality through the modification of magnetic and electronic behavior. Cobaltites display a range of spin state configurations, depending on the structure, doping, valence, pressure, and temperature. $LaCoO_3$ (LCO), like other undoped cobaltites, exhibits no long-range magnetic order, although the competition between the crystal field splitting and Hund's coupling leads to a mixture of possible Co high spin (HS, S=2), low spin (LS, S=0) and intermediate spin (IS, S=1) states[3,4] above ∼30 K. The different spin states can be accessed by changing temperature, the Co-O bond length through the use of hydrostatic pressure,[5–7] or the Co-O-Co bond angle through chemical pressure, i.e. substitution of La with a smaller rare-earth cation.[8] More recently, lattice distortions altering the spin state[9–15] or defect-induced changes to the valence state of the Co ions[15–17] have also been cited as possible sources of HS Co ions to explain the observed ferromagnetism in heteroepitaxially strained LCO thin films.

Epitaxial films of $PrCoO_3$ (PCO), serve as a model system in which we can explore the effects of substitution of La^{3+} with Pr^{3+} in a $4f^2$ state and also modify the magnitude of the spin gap. Bulk paramagnetic PCO has a smaller pseudocubic (pc) lattice parameter and an orthorhombically-distorted perovskite structure (a_{pc} ∼3.789 Å) compared to bulk LCO (rhombohedrally-distorted a_{pc} ∼3.81 Å), due to the smaller ionic size of Pr^{3+}. The chemical pressure thus decreases Co-O-Co bond angles, leading to a narrower e_g-derived bandwidth and a larger spin gap in bulk. This enhances the stability of the LS state relative to LCO, resulting in a shift of the onset of the spin state transition from about 30 K in LCO to above 200 K in PCO.[8] Tensily-strained epitaxial films may destabilize this LS state and instead promote the HS state, as the observation of ferromagnetism in LCO thin films would suggest.[9–15] Studies of PCO thin films could thus provide a first step in the direction of understanding the influence of the spin gap on ferromagnetic ordering in epitaxial films.

We demonstrate an emergent ferrimagnetic ground state in heteroepitaxial PCO thin films, where magnetic moment ordering occurs on both the Co *and* Pr sites. We find that the Co sublattice orders ferromagnetically, with significant evidence for HS Co, and it is aligned antiparallel to the ordered Pr sublattice. This is significant as ordering of Pr ions has not been observed in bulk cobaltites. The Pr ordering antiparallel to the Co ions accounts for the lower saturation magnetization for these PCO films compared to LCO films. We also observe a lower Curie temperature (T_C), likely due to the greater stability of the low spin state in bulk PCO. The ferromagnetic exchange mechanisms used to explain the behavior of metallic alkaline-earth doped bulk cobaltites is inconsistent with the insulating behavior of the PCO films obtained here. The apparently different mechanism for ferromagnetism in these films may facilitate strong exchange coupling between Pr and Co. These findings are significant since they set these thin films apart from other cobaltites, and they represent the first evidence of an interaction of this type between high spin Co ions and rare earth ions which result in novel ferrimagnetic behavior.

To probe the role of epitaxy on the spin state in PCO, we grew ∼8, ∼23 and ∼115 nm thick PCO films on (001) $SrTiO_3$ STO) and Nb-doped $SrTiO_3$ (lattice mismatch ∼3.0% for both) substrates by pulsed laser deposition (248 nm KrF excimer laser, ∼1 J/cm^2). A PCO polycrystalline target was synthesized by solid state reaction of stoichiometric quantities of Pr_6O_{11} (Sigma-Aldrich, 99.9% purity) and Co $(C_2O_4)\cdot 2H_20$ (Sigma-

Aldrich) powders. The reactants were thoroughly ground and reacted at 1000°C in air for 7 days, with 2 intermediate grindings. The reacted powder was cold-pressed into a disk at ∼16,000 psi and sintered at 1200°C in air for 96 hours. After cooling the target to room temperature at 0.5 °C/min, the phase purity was confirmed by X-ray diffraction. The films were grown with a laser pulse rate of 3 Hz in 320 mTorr of O_2 at 650°C-700°C and cooled in 10 Torr of O_2.

PCO films grown on both types of STO substrates exhibit good crystallinity with the full-width at half-maximum of the (002) rocking curves (or ω scans) of $\Delta\omega < 0.3°$ for films thinner than 25 nm and $\Delta\omega < 0.7°$ for thicker films. All PCO films exhibit low surface roughness with typical RMS values of 2.5 Å to 5 Å on a 5 μm lateral length scale. Reciprocal space maps around the (013) film and substrate peaks show that the 8 nm film is coherently strained to the substrate (Fig. 1(a)). As the PCO film thickness is increased (Fig. 1(b)), the in-plane film lattice parameter shifts from the substrate value (a_{pc} = 3.905 Å) towards the bulk PCO value of 3.79 Å, indicating film relaxation. At 115 nm thickness (Fig. 1(c)) there is almost full relaxation.

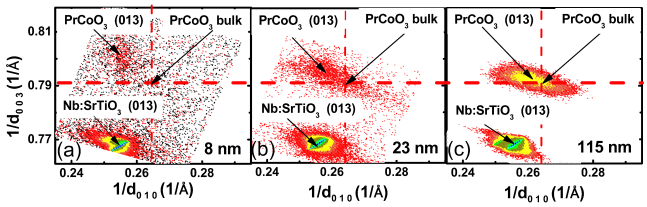

FIG. 1: (color online) Reciprocal space maps of the (013) reflection for a) 8 nm, (b) 23 nm and (c) 115 nm thick $PrCoO_3$ films grown on Nb-doped $SrTiO_3$ substrates.

All PCO films exhibited long-range magnetic order. In order to obtain accurate magnetization values, a high field negative slope background was subtracted from the data to eliminate diamagnetic and paramagnetic substrate contributions to the magnetic signal. The magnetization versus field loops, with magnetic fields applied in-plane, show magnetic hysteresis (Fig. 2(a)). Fig. 2(a) shows that the saturation magnetization does not scale in a simple manner with thickness. We find the highest saturation magnetization (∼0.4 μ_B/$PrCoO_3$ formula unit) for the thinnest films and observe a rapid drop in the magnetization with increasing thickness, eventually falling below ∼0.1 μ_B/$PrCoO_3$. Fig. 2(b) shows the magnetization dependence on temperature. These curves have been normalized to their low temperature values to enable facile comparison of the T_Cs. The 8 nm thick film has a T_C of ∼60 K, while the thicker films show a significant decrease in the T_C to around 40 K for the 115 nm thick film. This apparent decrease in T_C for the films of increasing thickness is likely related to the increasing degree of relaxation and can be understood as a decrease in the presence of HS Co. All films show a monotonic decrease in magnetization with increasing temperature.

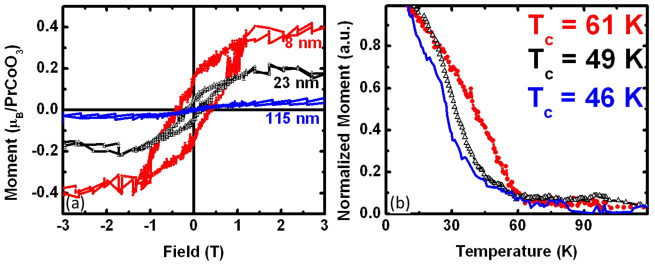

FIG. 2: (color online) (a) Magnetization versus magnetic field at 5 K and (b) magnetization versus temperature after field cooling and applying a static field of 5 mT for $PrCoO_3$ films 8, 23, and 115 nm thick.

This is important in the context of our finding of ferrimagnetism (see below), as it indicates that the Pr ordering temperature is close, or identical, to the Co ordering temperature.

The long-range magnetic order was further probed on a similar set of PCO films 8 nm and 110 nm thick by element-specific X-ray magnetic circular dichroism (XMCD) performed in total electron yield mode at the Advanced Light Source (beamlines 4.0.2 and 6.3.1) in 30° grazing incidence at 25 K. A 0.5 T magnetic field was applied in-plane to enable comparison with the in-plane SQUID measurements. Since transport measurements revealed PCO film samples to be insulating (consistent with prior work on LCO films),[16] for these measurements we used samples grown on conductive Nb-doped STO to help prevent charging. The X-ray absorption (XA) and XMCD spectra for 8 and 110 nm PCO films show differences as discussed below. XMCD spectra are descibed in terms of the difference in XA spectra measured with different relative orientations of photon spin and magnetic moment. XMCD signals are found at both the Co $L_{2,3}$ ($2p$ to $3d$) and Pr $M_{4,5}$ ($3d$ to $4f$) absorption edges, thus indicating that the ferromagnetism comes from both Co and Pr. The spectra from our films are compared to spectral results in literature[18–21] to provide insight into the films' spin state, valence, and site symmetry.[22]

The XA line shapes in Fig. 3(a) for the Co edge of the 8 nm (red open circles) and 110 nm (green solid triangles) PCO films indicate a greater presence of HS Co^{3+} in the thinner films. For comparison, we show spectra from Hu *et al.*[18] of bulk Sr_2CoO_3Cl and bulk $EuCoO_3$ (Fig. 3(a) orange solid squares and black crosses) which are known to have 100% HS and 100% LS respectively. Although these two compounds do not have identical Co coordination (i.e., pyramidal in Sr_2CoO_3Cl and octahedral in $EuCoO_3$), comparison of the two spectra suggests (i) an increase in the ratio of the L_3 pre-edge (A) intensity to the L_3 post-edge (C) intensity, (ii) a decrease in the ratio of the L_2 peak (D) intensity to the L_2 post-edge (E) intensity, and (iii) an increase in the ratio of the L_3 peak (B) intensity to the L_2 peak (D) intensity are indicative of a greater fraction of HS state Co. The 8 nm PCO film spectrum has features similar to (i), (ii), and (iii) thus

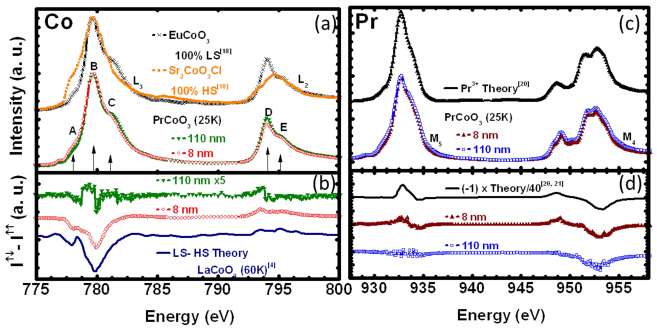

FIG. 3: (color online) XA (a,c) and XMCD (b,d) spectra at the Co $L_{2,3}$ (a,b) and the Pr $M_{4,5}$ (c,d) edges measured using circularly polarized X-rays and magnetic fields up to 0.5 T.

the film contains some HS Co^{3+}, while the 110 nm PCO film spectrum has features that are very similar to the 100% LS Co^{3+} in the $EuCoO_3$ reference.

The small feature at 777 eV is likely due to the presence of some small amount of Co^{2+} which suggests the presence of some oxygen vacancies in these films. The spectral features in our spectra could be fit by a combination of LS and HS Co^{3+} ions and a minor contribution from HS Co^{2+}, similar to what is observed in $LaCoO_3$ epitaxial systems.[23] The contribution of this small quantity of Co^{2+} to the XA spectra does not fully account for the net moment through the entire film. In addition, this feature is present in both thin and thick films and shows little change as a function of applied field indicating a weaker correlation with the films' overall magnetic behavior.

The Co XMCD for the 8 nm PCO film Fig. (3(b) red open circles) is stronger than for the 110 nm film Fig. (3(b) green solid triangles). The paramagnetic dichroism[4] calculated for a small population of HS Co^{3+} under a 6 T field on single crystal LCO at 60 K Fig. (3(b) dark blue line) shows similar features (though not identical) to the XMCD of our samples. The dichroism signal from the thick sample is lower, consistent with SQUID magnetometry, and as a result has a lower signal to noise ratio. We also found that the XMCD dependence with temperature (not shown) for the 8 nm film was consistent with SQUID magnetometry showing magnetic dichroism below 50 K and none above 175 K. Since dichroism signals from both films, using the convention $I^{\uparrow\downarrow}-I^{\uparrow\uparrow}$, match the dichroism sign changes in the paramagnetic LCO reference, we can conclude that the Co moment is aligned with the applied magnetic field.

Our XA spectra at the Pr M edge Fig. (3(c)) are characteristic of Pr^{3+} and are similar to the calculated spectrum.[20] We observe no evidence of charge transfer or features associated with Pr^{4+}, unlike the bond-length changes and strong $4f$-$2p$ hybridization that has been observed for bulk $Pr_{0.5}Ca_{0.5}CoO_3$.[19] Calculated dichroism features of Pr^{3+} at the $M_{4,5}$ edge[20,21] match features in the experimental spectrum in both relative magnitude and energy (see Fig. 3(d)), but not in sign, confirming magnetism arising from the Pr^{3+} ions and their antiparallel orientation to the Co^{3+} moment and the applied field. The Pr XMCD is also stronger for the 8 nm film Fig. (3(d) dark red solid triangles) than for the 110 nm PCO film Fig. (3(d) blue open squares).

The magnetic field dependence of the XMCD signal at the Co and Pr edges provides insight into the switching behavior of Co and Pr. Due to the measurement conditions these loops only provide qualitative information regarding the relative switching of Pr and Co. Fig. 4(a) and 4(b) show element specific hysteresis loops taken at 779.9 eV for Co (the L_3 peak) and at 953.1 eV for Pr (the M_4 peak) as a function of field. The dichroism for the 8 nm film shows clear hysteresis (Fig. 4(a)) indicating that both the Co and Pr are ferromagnetic. The thicker 110 nm film (Fig. 4(b)) shows no clear hysteresis and a reduced dichroism at both Co and Pr edges, thus indicating much weaker ferromagnetism. During our investigations, we also observed that this reducd dichroism trend with thickness held true for a ∼25 nm thick PCO film as well (omitted in this work). We observed a lower (higher) magnetic Co and Pr dichroism in a ∼25 nm sample compared to the ∼8 nm (∼110 nm) sample.

From the data, there is a strong correlation between tensile strain and ferromagnetism in the films. Very thin PCO films under coherent tensile strain have tetragonal unit cell symmetry and show ferromagnetic behavior with a $T_C \leq 60$ K. As the thickness is increased, and the structure becomes more cubic and akin to bulk PCO, the magnetic moment is diminished and the T_C decreases. Combined with the XA evidence for high spin Co in the thinner PCO films, this trend in the magnetism suggests that we stabilize long-range magnetic order and HS cobalt via epitaxial tensile strain. We speculate that the lattice distortions arising from epitaxy correspond to a decrease in the overall crystal field splitting and possibly a change in the distribution of electronic energy levels compared to the bulk. In bulk PCO, the LS state of S=0 is stable up to 200 K, which is a much higher temperature compared to bulk LCO (spin state transition occurs at ∼30 K). The decreased orbital overlap and hybridization due to the smaller Co-O-Co bond angles in bulk PCO, aid the stabilization of the LS state.[8] Given the increased stability of the Co LS state in bulk PCO, it is noteworthy that we observe any long-range magnetic order in PCO films. Distortion of the lattice in the tensily strained films appears to oppose the smaller Co-O-Co bond angles and alters the crystal field enough to partially drive the system to a HS state. Epitaxial tensile strain and chemical pressure from the smaller Pr cation represent competing influences on the spin state stability. Thus the long-range order suggests that lattice changes from epitaxy dominate or overwhelm the decreasing bond-angle tendencies (from 164° in bulk LCO to ∼157°[24] in bulk PCO) caused by the Pr chemical pressure on the Co octahedra. However, the reduction in T_C (∼60 K for PCO films compared to 80 K for LCO films)[9] suggests that the smaller Pr cation does, to some extent, reduce the

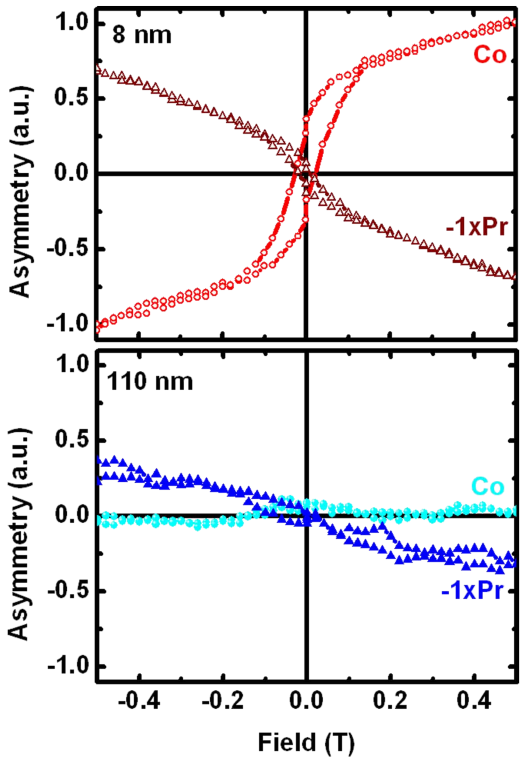

FIG. 4: (color online) Element specific hysteresis loops taken at 25 K for thin (a) and thick (b) $PrCoO_3$ films on Nb-doped $SrTiO_3$ substrates show a different field dependence.

strength of the orbital overlap that gives rise to the ferromagnetic exchange between Co ions.

The most remarkable finding of this investigation however is the demonstration of two ferromagnetic sublattices: one of Co ions aligning with the applied magnetic field and another of Pr ions that is antiferromagnetically coupled to the Co moments. This reveals that these films are more appropriately described as ferrimagnetic and display a monotonic temperature dependence with a T_C of ∼60 K. Pr^{3+} ions in bulk PCO do not show any ordering down to 4 K.[25] In doped $Pr_{1-x}Sr_xCoO_3$, long-range ferromagnetism associated with the Co ions is observed for x > 0.2[26] and can be attributed to the double exchange interaction among IS Co moments in an intermediate valence, mediated by a mobile e_g electron. Features in the magnetism have been associated with an abrupt change in the magnetic anisotropy and a dramatic structural change,[26–28] associated with strong Pr $4f$-O $2p$ orbital hybridization below 120 K.[26,29] However, in contrast to the findings in our work, Pr ordering does not occur even in these doped bulk systems.[26] In undoped systems, despite the tendency for a singlet state, Pr^{3+} magnetic ordering could occur provided the exchange in the vicinity of the ions is strong enough.[30] However, in previously studied undoped perovskites,[31–33] the Pr^{3+} ions have only shown to be weakly exchange coupled to the transition metal ions with no tendency for ferrimagnetic ordering.

In our epitaxially strained films, the Pr moment appears to be strongly coupled to the HS/LS Co moments, unlike the bulk $Pr_{1-x}Sr_xCoO_3$ IS Co scenario. Thus, the stabilization of ferrimagnetism and insulating behavior here presents a unique behavior not observed in other Pr-based perovskite oxides. Presumably, the larger ionic size and the higher spin moment of HS Co ions contribute to the Pr magnetic site ordering by increasing the possibility for strong Pr-Co exchange.[30] However, we do not observe any evidence for increased Pr-O hybridization from the XA spectra, unlike in the $Pr_{1-x}Ca_xCoO_3$[19] and $Pr_{1-x}Sr_xCoO_3$ systems.[26] The prior work exploring relevant crystal field effects in Pr-containing perovskites focuses on cubic or very close to cubic symmetry. In these epitaxial films we stabilize tetragonal symmetry which may also play some role in enabling Pr ordering. In any case, the ordering of Pr observed here is fundamentally different from the high T_C IS Co system (alkaline-earth doped PCO) where no Pr ordering is observed. In our study, the transition temperature for both HS Co ions and Pr ions is the highest ordering temperature reported thus far for a Pr sublattice and is evidence that the ordering of Co and Pr occur together.

In summary, we have stabilized ferrimagnetic PCO thin films composed of antiparallel Co and Pr ferromagnetic sublattices that simultaneously order with a T_C ≤60 K. The epitaxial lattice strain overwhelms the competing chemical pressure effects from the smaller Pr cation to stabilize a low temperature HS ground state in the Co ion. This insulating ferrimagnetism is fundamentally different from the double exchange interaction found in doped cobaltites and can be attributed to strong exchange among HS Co ions and Pr ions. It thus appears that capitalizing on the HS/LS Co-based magnetism in cobaltite films may offer a new route to higher temperature magnetic ordering of rare-earth ions.

This work was supported by the Director, Office of Science, Office of Basic Energy Sciences, Division of Materials Science and Engineering as well as Scientific User Facilities Division of the U.S. Department of Energy under Contract No. DE-AC02-05CH11231. Work at UMN was supported by the NSF and DOE (scattering characterization). We thank K. M. Yu for help with RBS, and F. Wong, A. Grutter, and U. Alaan for discussions.

[1] R. R. Heikes, R. C. Miller, and R. Mazelsky, Physica **30**, 1600 (1964)

[2] P. M. Racah and J. B. Goodenough, Phys. Rev. **155**,932 (1967)

[3] M. A. Korotin, S. Y. Ezhov, I.V. Solovyev, V. I. Anisimov, D. I. Khomskii, and G. A. Sawatzky, Phys. Rev. B **54**, 5309 (1996)

[4] M. W. Haverkort, Z. Hu, J. C. Cezar, T. Burnus, H. Hartmann, M. Reuther, C. Zobel, T. Lorenz, A. Tanaka, N. B. Brookes, H. H. Hsieh, H. -J. Lin, C. T. Chen, and L. H. Tjeng, Phys. Rev. Lett. **97**, 176405 (2006)

[5] G. Vanko, J. -P. Rueff, A. Mattila, Z. Nemeth, and A. Shukla, Phys. Rev. B **73**, 024424 (2006)

[6] T. Vogt, J. A. Hriljac, N. C. Hyatt, and P. Woodward, Phys. Rev. B **67**, 140401 (2003)

[7] D. P. Kozlenko, N. O. Golosova, Z. Jirak, L. S. Dubrovinsky, B. N. Savenko, M. G. Tucker, Y. Le Godec, and V. P. Glazkov, Phys. Rev. B **75**, 064422 (2007)

[8] M. Tachibana, T. Yoshida, H. Kawaji, T. Atake, and E. Takayama-Muromachi, Phys. Rev. B **77**, 094402 (2008)

[9] D. Fuchs, C. Pinta, T. Schwarz, P. Schweiss, P. Nagel, S. Schuppler, R. Schneider, M. Merz, G. Roth, and H. v. Lhneysen, Phys. Rev. B **75**, 144402 (2007)

[10] D. Fuchs, E. Arac, C. Pinta, S. Schuppler, R. Schneider, and H. v. Loehneysen, Phys. Rev. B **77**, 014434 (2008)

[11] D. Fuchs, L. Dieterle, E. Arac, R. Eder, P. Adelmann, V. Eyert, T. Kopp, R. Schneider, D. Gerthsen, and H. v. Loehneysen, Phys. Rev. B **79**, 024424 (2009)

[12] A. D. Rata, A. Herklotz, L. Schultz, and K. Dorr, The Eur. Phys. J. B **76**, 215 (2010)

[13] A. Herklotz, A. D. Rata, L. Schultz, and K. Dorr, Phys. Rev. B **79**, 092409 (2009)

[14] V. Mehta and Y. Suzuki, J. Appl. Phys. **109**, 07D717 (2011)

[15] S. Park, P. Ryan, E. Karapetrova, J. W. Kim, J. X. Ma, J. Shi, J. W. Freeland, and W. Wu, Appl. Phys. Lett. **95**, 072508 (2009)

[16] J. W. Freeland, J. X. Ma, and J. Shi, Appl. Phys. Lett. **93**, 212501 (2008)

[17] V. Mehta and Y. Suzuki, J. Appl. Phys. **109**, 07D717 (2011)

[18] Z. Hu, H. Wu, M. W. Haverkort, H. H. Hsieh, H. J. Lin, T. Lorenz, J. Baier, A. Reichl, I. Bonn, C. Felser, A. Tanaka, C. T. Chen, and L. H. Tjeng, Phys. Rev. Lett. **92**, 207402 (2004)

[19] J. Herrero-Martin, J. L. Garcia-Munoz, S. Valencia, C. Frontera, J. Blasco, A. J. Baron-Gonzalez, G. Subias, R. Abrudan, F. Radu, E. Dudzik, R. Feyerherm, Physical Review B **84**, 115131 (2011)

[20] J. B. Goedkoop, B. T. Thole, G. van der Laan, G. A. Sawatzky, F. M. F. de Groot, and J. C. Fuggle, Physical Review B 37, 2086 (1988)

[21] G. van der Laan, E. Arenholz, Z. Hu, A. Bauer, E. Weschke, Ch. Schussler-Langeheine, E. Navas, A. Muhlig, G. Kaindl, J. B. Goedkoop, and N. B. Brookes, Physical Review B **59**, 8835 (1999)

[22] M. Abbate, J. C. Fuggle, A. Fujimori, L. H. Tjeng, C. T. Chen, R. Potze, G. A. Sawatzky, H. Eisaki, and S. Uchida, Physical Review B **47**, 16124 (1993)

[23] M. Merz, P. Nagel, C. Pinta, A. Samartsev, H. v. Lohneysen, M. Wissinger, S. Uebe, A. Assmann, D. Fuchs, S. Schuppler, Physical Review B **82**, 174416 (2010)

[24] K. Knizek, Jiri Hejtmanek, Zdenek Jirak, Petr Tomes, Paul Henry, and Gilles Andre, Physical Review B **79**, 134103 (2009)

[25] I. G. Deac, R. Tetean, I. Balasz, and E. Burzo, J. Magn. Magn. Mater. **322**, 1185 (2010)

[26] C. Leighton, D. D. Stauffer, Q. Huang, Y. Ren, S. El-Khatib, M. A. Torija, J. Wu, J. W. Lynn, L. Wang, N. A. Frey, H. Srikanth, J. E. Davies, K. Liu, and J. F. Mitchell, Phys. Rev. B **79**, 214420 (2009)

[27] M. Uchida, R. Mahendiran, Y. Tomioka, Y. Matsui, K. Ishizuka, and Y. Tokura, Appl. Phys. Lett. **86**, 131913 (2005)

[28] S. Hirahara, Y. Nakai, K. Miyoshi, K. Fujiwara, and J. Takeuchi, J. Magn. Magn. Mater. **310**, 1866 (2007)

[29] I. O. Troyanchuk, D. V. Karpinskii, A. N. Chobot, D. G. Voitsekhovich, and V. M. Dobryanskii, JETP Lett. **84**, 151 (2006)

[30] Y. Wang, and B. Cooper, Phys. Rev. **172**, 539 (1968)

[31] J. D. Gordon, R. M. Hornreich, S. Shtrikman, and B. M. Wanklyn, Phys. Rev. B **13**, 3012 (1976)

[32] A. A. Mukhin, V. Yu, V. D. Travkin, A. M. Balhashov, J. Magn. Magn. Mater. **226-230**, 1139 (2001)

[33] X. Wang, S. Cao, Y. Wang, S. Yuan, B. Kang, A. Wu, and J. Zhang, J. Crys. Growth, Jan. (2012). (in press) DOI:10.1016/j.jcrysgro.2011.12.096